ARTICLE

Effects of Hydrogen Plasma Treatment on the Electrical and Optical Properties of ZnO Films: Identification of Hydrogen Donors in ZnO

J. J. Dong,[†] X. W. Zhang,*[,†] J. B. You,[†,‡] P. F. Cai,[†] Z. G. Yin,[†] Q. An,[†] X. B. Ma,[‡] P. Jin,[†] Z. G. Wang,[†] and Paul K. Chu[‡]

Key Lab of Semiconductor Materials Science, Institute of Semiconductors, Chinese Academy of Science, Beijing 100083, People's Republic of China, and Department of Physics and Materials Science, City University of Hong Kong, Tat Chee Avenue, Kowloon, Hong Kong, People's Republic of China

ABSTRACT Wurtzite ZnO has many potential applications in optoelectronic devices, and the hydrogenated ZnO exhibits excellent photoelectronic properties compared to undoped ZnO; however, the structure of H-related defects is still unclear. In this article, the effects of hydrogen-plasma treatment and subsequent annealing on the electrical and optical properties of ZnO films were investigated by a combination of Hall measurement, Raman scattering, and photoluminescence. It is found that two types of hydrogen-related defects, namely, the interstitial hydrogen located at the bond-centered (H_{BC}) and the hydrogen trapped at a O vacancy (H_O), are responsible for the n-type background conductivity of ZnO films. Besides introducing two hydrogen-related donor states, the incorporated hydrogen passivates defects at grain boundaries. With increasing annealing temperatures, the unstable H_{BC} atoms gradually diffuse out of the ZnO films and part of them are converted into H_O, which gives rise to two anomalous Raman peaks at 275 and 510 cm^{-1}. These results help to clarify the relationship between the hydrogen-related defects in ZnO described in various studies and the free carriers that are produced by the introduction of hydrogen.

KEYWORDS: hydrogen plasma treatment • zinc oxide • Raman spectroscopy • photoluminescence

INTRODUCTION

Wurtzite ZnO has many potential applications in optoelectronic devices because of its large band gap of 3.37 eV as well as high exciton binding energy of 60 meV at room temperature (RT) (1, 2). It is considered as the most promising material for light-emitting diodes (LEDs) and laser diodes (LDs). However, nominally undoped ZnO typically exhibits n-type conductivity and this background n-type conduction precludes effective p-type doping due to hole compensation by donors. The nature of this conductivity has been widely discussed for years and is normally attributed to native defects, such as the oxygen vacancy (V_O) and the Zn interstitial (Zn_i) (1, 2). Recently, unintentionally incorporated hydrogen (H) is considered as a likely source of the n-type conductivity of ZnO (3), and H-related defects in ZnO have attracted great interest and been extensively studied (3−22) because of their profound effects on the electrical properties of ZnO. Three H states can hitherto be found in a ZnO crystal (16). The first one is the interstitial H (H_i), which can be located at the bond-centered (H_{BC}) or the antibonding (H_{AB}) site of the ZnO lattice by the formation of O−H bond (3, 11). The second one corresponds to the H attached to defects. For example, H can be trapped at a O vacancy to form V_O−H complex (also called as H_O) (13, 20) or Zn vacancy to form (V_{Zn}−H_2) complex (5, 16). The last one is the loose (unbound) H, which occurs in the form of interstitial H_2 (21). Many studies have confirmed that H is a shallow donor in ZnO; however, the experimental data for H in ZnO remain puzzling (8, 14, 18−20). It has been reported that the isolated H_i acts as shallow donors in ZnO (3, 14, 15); however, several possible configurations of H_i in ZnO have similar formation energies and their thermal stability is found to be low (11, 13). On the other hand, the H_i bonded to Zn-site transition metals (9) and the H_O (12−14, 17) have also been suggested to be shallow donors. Despite years of investigations, the structure of H-related defects is still controversial. Therefore, it is imperative that experiments be conducted to confirm the assignment.

In this article, the effects of H-plasma treatment and subsequent annealing on the electrical and optical properties of ZnO films are studied by Hall measurement, Raman scattering, and photoluminescence (PL). It is found that two types of H-related defects, namely, the H_i and the H_O, are responsible for the *n*-type background conductivity of ZnO films.

EXPERIMENTAL SECTION

Preparation Process of ZnO Films. The ZnO films were deposited on c-plane sapphire substrates by a conventional radio frequency (rf) magnetron sputtering system equipped with a ZnO (99.99%) ceramic target. The sputtering chamber was evacuated to a base pressure of 1.0×10^{-5} Pa, and then filled with the working gas (pure Ar) to a pressure of 1.0 Pa. Prior to

* To whom correspondence should be addressed. E-mail: xwzhang@semi.ac.cn.

Received for review April 2, 2010 and accepted May 18, 2010

† Chinese Academy of Science.

‡ City University of Hong Kong.

DOI: 10.1021/am100298p

Published on Web 05/25/2010

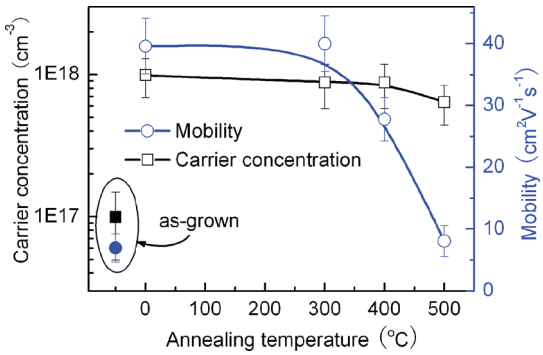

FIGURE 1. Variation in the carrier concentration and mobility as a function of the annealing temperature for the H-plasma-treated ZnO films. For comparison, the corresponding data of the as-grown ZnO film is also included.

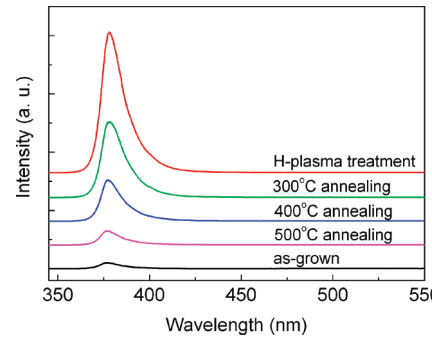

FIGURE 2. RT PL spectra of the as-grown, H-plasma-treated, and subsequently annealed ZnO films.

deposition, the substrates were sequentially cleaned in the ultrasonic baths of acetone, ethanol, and deionized water, and then blown dried with nitrogen gas. The films were deposited at 600 °C with a constant rf power of 80 W for 2 h, and the sapphire substrates were placed on the substrate holder at a distance of 80 mm from the target. To introduce H intentionally, we directly immersed the ZnO films in a H-plasma in a capacitively coupled plasma reactor. During the plasma treatment, the rf power and the working pressure were kept at 70 W and 200 Pa, respectively. Details of growth and treatment conditions can be found elsewhere (19). In the present study, the thickness of the ZnO films is about 1 μm, hence H can diffuse into the entire film, as demonstrated by secondary ion mass spectroscopy (SIMS) (22). To investigate the thermal stability of H in ZnO, we annealed the H-plasma treated ZnO films at various temperatures in a vacuum for 2 h.

Characterization. The carrier concentration and mobility of the ZnO films were determined by Hall measurements using the Van der Pauw configuration. For the Hall measurements, Ti/Au (50/100 nm) was used as an Ohmic contact metal. The PL spectra were acquired by exciting with a 325 nm He−Cd laser with a power of 30 mW at both RT and 10 K by using a photomultiplier tube detector. Raman scattering measurements were carried out at RT using the 514.5 nm excitation lines from an Ar ion laser and a Horiba HR800 spectrometer in the backscattering geometry.

RESULTS AND DISCUSSION

It has been reported that H-doping significantly decreases the resistivity of ZnO, however, the resistivity data alone cannot precisely distinguish between H present as an isolated donor or passivating an acceptor impurity or native defect. The electrical properties of the ZnO films after the H-plasma treatment and subsequent annealing at different temperatures were studied in detail in terms of the carrier concentration and mobility. As shown in Figure 1, the as-grown ZnO film possesses a high resistivity with the carrier concentration and mobility being about 1×10^{17} cm^{-3} and 7 cm^2 V^{-1} s^{-1}, respectively. After 2 h of H-plasma exposure, both values increase sharply. The carrier concentration goes up to 1×10^{18} cm^{-3} for and the mobility reaches 39 cm^2 V^{-1} s^{-1}. On the one hand, the remarkable increase in the carrier concentration indicates the formation of a shallow donor level as a result of H incorporation into the ZnO film. On the other hand, the simultaneous increase in mobility suggests that in addition to shallow donors, a substantial fraction of the incorporated H passivates defects at grain boundaries, because the higher carrier concentration usually leads to strong carrier scattering and reduced mobility. Therefore, the incorporated H not only introduces a shallow donor state, but also passivates most of the defects at grain boundaries. It is possible that the introduced H acts at grain boundaries to passivate the defects, such as dangling bonds. As a result, the mobility increases because of a decrease in the intergrain barrier height and a narrowing of the depletion layer at the grain boundaries due to the screening effect by free electrons (23). Our observations are consistent with the previous findings (6, 19, 23).

To investigate the thermal stability of H in ZnO, the H-plasma treated ZnO films were annealed at 300, 400, and 500 °C in a vacuum for 2 h, respectively. As shown in Figure 1, the carrier concentration decreases slightly with annealing temperature, from 1×10^{18} cm^{-3} for the H-plasma treated ZnO to 6.5×10^{17} cm^{-3} for the 500 °C annealed sample, implying the out-diffusion of partial H-related donors from ZnO. Furthermore, the carrier concentration in the 500 °C annealed ZnO is still much higher than that of the as-grown sample, indicating that most of the shallow donors introduced by H are stable up to 500 °C. On the other hand, the mobility of the ZnO films remains almost constant at the annealing temperature of 300 °C and then decreases sharply to a value close to that of the as-grown sample, suggesting that all of the H passivating the defects at grain boundaries evolve out of the ZnO films at 500 °C.

Figure 2 shows the RT PL spectra of the as-grown, H-plasma treated and subsequent annealed ZnO films, respectively. After the H-plasma treatment, the intensity of the ZnO ultraviolet (UV) emission is enhanced by more than twenty times. Similar results have been reported, with the observations on the suppression of visible emission from ZnO by H-plasma treatment (4, 10). Furthermore, it has also been reported that unintentional incorporation of H during the Ar plasma treatment also resulted in a significant enhancement of the ZnO UV emission (24). In the present work, no evidence of the existence of visible emission is observed because of the higher quality of the ZnO films. The intensity of the UV emission decreases gradually with increasing annealing temperature, and at 500 °C it is 2.5 times higher than that of the as-grown ZnO film.

To further understand the structure of H-related defects, we also measured the near band-edge emission (NBE) PL spectra at 10 K. As shown in Figure 3, the luminescence at

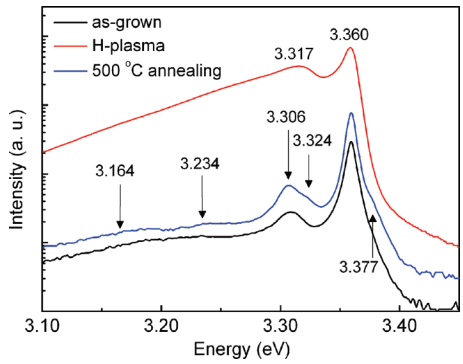

FIGURE 3. PL spectra of the as-grown, H-plasma-treated, and 500 °C annealed ZnO films measured at 10K.

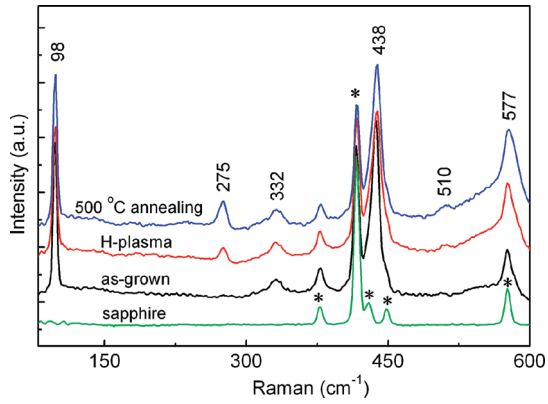

FIGURE 4. RT Raman spectra of the sapphire substrate as well as as-grown, H-plasma treated and 500 °C annealed ZnO films. The peaks marked by asterisks originate from the sapphire substrate.

10 K from all three samples is dominated by the neutral-donor bound-exciton (D^0X) emission at 3.360 eV. The PL spectra obtained from the as-grown and subsequent annealed ZnO films show a weak free exciton (FX) emission at 3.377 eV, which is the shoulder of the D^0X. Besides the D^0X and FX peaks, three emission lines at 3.306, 3.234, and 3.164 eV are observed in both spectra. They are the first-, second- and third-order LO-phonon replicas of the FX emission (FX-1LO, FX-2LO and FX-3LO), respectively (1, 25, 26). After the H-plasma treatment, the D^0X peak is enhanced by more than twenty times, whereas the FX peak is suppressed completely. Obviously, not only the free excitons are bound to the H-related shallow donors, but also the nonradiative defects at grain boundaries are passivated by the introduced H. Furthermore, two additional emission lines at 3.317 and 3.324 eV emerge from the H-plasma treated and subsequently annealed ZnO films, respectively, which are attributed to the two-electron satellite (TES) transitions and will be discussed in detail later.

To shed further light on the role of H in ZnO, Raman spectra were acquired at RT and the results are presented in Figure 4, which also includes the Raman spectrum of the sapphire substrate for comparison. Five Raman peaks of sapphire located at 378, 416, 429, 448, and 576 cm^{-1} are observed from the substrate (27). Besides the Raman peaks originating from the substrate, there are four photon modes of ZnO at 98, 332, 438, and 577 cm^{-1} labeled as E_2 (low), E_2 (high)-E_2 (low), E_2 (high), and A_1 (LO), respectively (28−30). The most important feature, however, of the results presented in this figure, is the fact that two new Raman peaks at 275 and 510 cm^{-1}, which do not belong to first- or second-order structures of ZnO, are observed from the H-plasma-treated and annealed samples. These anomalous peaks have been observed from doped ZnO films (30−35). In earlier studies, because the intensity of these additional modes correlates linearly with the N concentration, these modes were interpreted in terms of N-related local vibrational modes (30−33). Bundesmann et al. (34) reported that the anomalous peaks at 277 and 511 cm^{-1} also existed in the spectra of Fe-, Sb-, and Al-doped ZnO thin films. They attributed the common anomalous peaks to intrinsic host-lattice defects related to doping because most of the peaks observed after N doping were also observed from other doped samples. Recently, by comparing previous experimental results with reported calculations of the lattice dynamics in ZnO (36), Manjón et al. (37) showed that the anomalous peaks corresponded to silent ZnO Raman modes observed by disorder-activated Raman scattering because of the relaxation of the Raman selection rules produced by the breakdown of the translational symmetry of the crystal lattice. Supported by refs 34−37, two observed Raman peaks at 275 and 510 cm^{-1} could be attributed to the B_1(low) and $2B_1$(low) ZnO silent modes activated by H-related defects, respectively. Although such anomalous Raman peaks have been observed for doped ZnO films with various elements, it is the first time to report the two peaks for the H-plasma-treated ZnO thin film.

A thorough comprehension of the nature of H in ZnO is essential in order to control doping and realize its applications. As reported in our previous work, the relative intensity and the full width at half-maximum (fwhm) of ZnO X-ray diffraction peaks are almost not changed, indicating that the crystallinity is not influenced after H plasma treatment (19). Furthermore, atomic force microscopy (AFM) images indicated that the surface roughness and morphologies of the ZnO films treated with H plasma are almost similar to those of the as-grown sample (22), while UV−vis measurements showed that the transmittance edge of the H-plasma treated ZnO film shifts to a slightly lower wavelength, which is due to the Burstein−Moss effect (19). On the basis of the observed results and the previous data, the effects of H on the ZnO properties can be tentatively understood by the following interpretation. On the one hand, after exposing ZnO films to the H-plasma, the improvement in the mobility and UV emission efficiency suggests the passivation of defect-related recombination centers. On the other hand, the remarkable increase in the carrier concentration indicates that in addition to passivation of the defects, the H-related shallow donors are formed. Evolution of the carrier concentration after annealing reflects the involvement of at least two different H-related defects, which are tentatively identified as H_i and H_O, respectively. First-principles calculations show that H_O is highly stable whereas H_i is unstable at high temperature (11, 13). The kinetic Montc Carlo simulations clearly indicates that H_O has a higher migration energy of

about 1.7 eV compared with 0.8 eV for H_i (18). Additionally, the appearance of a strong I_4 emission line after H implantation and the quenching of this I_4 line with time indicated the poor thermal stability of H_i, whereas a very stable quenching effect of the deep level emission implied that H_O have a much higher diffusion activation barrier (24). Therefore, we suppose that two types of shallow donors, H_i and H_O, are introduced by the H-plasma treatment. With increasing annealing temperatures, the unstable H_i atoms gradually diffuse out of the ZnO films and part of them are converted into H_O. Consequently, the H_O concentration increases gradually with annealing temperatures, which is also confirmed by the Raman and low temperature (LT) PL spectra. Although H_i diffuse out of the ZnO films with increasing annealing temperatures to 500 °C, the simultaneous increase of H_O lead to the relatively small changes in carrier concentrations with the variation of annealing temperature. On the other hand, the out-diffusion of H passivating defects at grain boundaries with annealing temperatures results in the drastically decrease in the intensities of the UV emission in the PL spectra.

Between the two configurations of H_i, H_{BC} is the more likely candidate since the formation energy of H_{BC} is lower than that of H_{AB} by 0.2 eV (3). An additional piece of evidence supporting the H_{BC} configuration is that the position of D^0X peak (3.360 eV) for the H-plasma treated sample is in agreement with the reported 3.3601 eV of H_{BC} (20). Furthermore, the TES transitions in the LT PL spectra may impart useful information to identify H-related donors in ZnO (25, 26). A TES transition occurs when an exciton bound to a neutral donor D^0X recombines and leaves the donor in an excited state. Therefore, the energy difference between the bound exciton line and the TES line corresponds to the energy difference between the excited and ground states of the donor. In the effective mass approximation, the donor excitation energy from the ground state (D^0X) to the first excited state (TES) is equal to 3/4 of the donor binding energy E_D (25, 26). According to the 3.360 eV D^0X and the corresponding 3.317 eV TES_1 lines, the value of E_{D1} is calculated to be 57 meV for the H-plasma treated film and it is close to the reported E_D of H_{BC} (53 meV) (20). On the basis of the 3.360 D^0X and the 3.324 eV TES_2 lines, the value of E_{D2} of the annealed sample is calculated to be 48 meV, which is in remarkable agreement with the reported E_D of H_O (47 meV) (20, 25, 26). Evidently, the 3.360 D^0X peak originates from the overlap of two bound-exciton emission lines of H_{BC} and H_O. After annealing, the out-diffusion of H_{BC} results in the disappearance of the TES_1 lines (H_{BC}).

Considering the electrical and PL results, it is believed that the Raman peaks at 275 and 510 cm^{-1} result from the H_O defects, which break down of the translational symmetry of the ZnO crystal lattice and activate the silent Raman modes of B_1(low). As discussed above, part of H_{BC} is converted into H_O during annealing and H_O is highly stable at 500 °C, therefore, the H_O concentration increases with annealing temperature. As shown in Figure 4 one can actually see that the intensities of the Raman peaks at 275 and 510 cm^{-1} increase after 500 °C annealing, reflecting the increase of the H_O concentration, which is in good agreement with the electrical and PL results. Furthermore, thermal stability of the H_O is also better than that of the H passivating the defects at grain boundaries, which evolves out of the ZnO films at 500 °C, because diffusion of H along the grain boundaries is relatively easy.

CONCLUSION

In conclusion, the effects of the H-plasma treatment and the subsequent annealing on the electrical and optical properties of ZnO thin films were investigated by a combination of several methods. The results indicate that the incorporated H atoms not only introduce shallow donor states, but also passivate most of the defects. Both H_{BC} and H_O are responsible for the n-type background conductivity of ZnO. With increasing annealing temperatures, the unstable H_i atoms gradually diffuse out of the ZnO films and part of them are converted into H_O, consequently, the concentration of H_O increases gradually with annealing temperatures. These results help to clarify the relationship between the H-related defects in ZnO described in various studies and the free carriers that are produced by the introduction of H.

Acknowledgment. This work was financially supported by the "863" project of China (Grant 2009AA03Z305), the National Natural Science Foundation of China (Grant 60876031, 60806044), the National Basic Research Program of China (Grant 2010CB933800), and Hong Kong Research Grants Council (RGC) General Research Funds (GRF) CityU 112608.

REFERENCES AND NOTES

(1) Özgür, Ü.; Alivov, Y. I.; Liu, C.; Teke, A.; Reshchikov, M. A.; Doğan, S.; Avrutin, V.; Cho, S. J.; Morkoç, H. *J. Appl. Phys.* **2005**, *98*, 041301.
(2) Pearton, S. J.; Norton, D. P.; Ip, K.; Heo, Y. W.; Steiner, T. *Prog. Mater. Sci.* **2005**, *50*, 293.
(3) Van de Walle, C. G. *Phys. Rev. Lett.* **2000**, *85*, 1012.
(4) Lee, J. M.; Kim, K. K.; Park, S. J.; Choi, W. K. *Appl. Phys. Lett.* **2001**, *78*, 3842.
(5) Lavrov, E. V.; Weber, J.; Börrnert, F.; Van de Walle, C. G.; Helbig, R. *Phys. Rev. B* **2002**, *66*, 165205.
(6) Seager, C. H.; Myers, S. M. *J. Appl. Phys.* **2003**, *94*, 2888.
(7) Strzhemechny, Y. M.; Nemergut, J.; Smith, P. E.; Bae, J.; Look, D. C.; Brillson, L. J. *J. Appl. Phys.* **2003**, *94*, 4256.
(8) Monakhov, E. V.; Kuznetsov, A. Y.; Svensson, B. G. *J. Phys. D: Appl Phys.* **2009**, *42*, 153001.
(9) Wardle, M. G.; Goss, J. P.; Briddon, P. R. *Phys. Rev. B* **2005**, *72*, 155108.
(10) Lin, C. C.; Chen, H. P.; Liao, H. C.; Chen, S. Y. *Appl. Phys. Lett.* **2005**, *86*, 183103.
(11) Wardle, M. G.; Goss, J. P.; Briddon, P. R. *Phys. Rev. Lett.* **2006**, *96*, 205504.
(12) Selim, F. A.; Weber, M. H.; Solodovnikov, D.; Lynn, K. G. *Phys. Rev. Lett.* **2007**, *99*, 085502.
(13) Janotti, A.; Van de Walle, C. G. *Nat. Mater.* **2007**, *6*, 44.
(14) Oh, M. S.; Hwang, D. K.; Lim, J. H.; Choi, Y. S.; Park, S. J. *Appl. Phys. Lett.* **2007**, *91*, 212102.
(15) Qiu, H.; Meyer, B.; Wang, Y.; Wöll, C. *Phys. Rev. Lett.* **2008**, *101*, 236401.
(16) Č|Aazek, J.; Žaludová, N.; Vlach, M.; Daniš, S.; Kuriplach, J.; Procházka, I.; Brauer, G.; Anwand, W.; Grambole, D.; Skorupa, W.; Gemma, R.; Kirchheim, R.; Pundt, A. *J. Appl. Phys.* **2008**, *103*, 053508.
(17) Li, Y. J.; Kaspar, T. C.; Droubay, T. C.; Zhu, Z.; Shutthanandan, V.; Nachimuthu, P.; Chambers, S. A. *Appl. Phys. Lett.* **2008**, *92*, 152105.

(18) Bang, J.; Chang, K. J. *Appl. Phys. Lett.* **2008**, *92*, 132109.
(19) Cai, P. F.; You, J. B.; Zhang, X. W.; Dong, J. J.; Yang, X. L.; Yin, Z. G.; Chen, N. F. *J. Appl. Phys.* **2009**, *105*, 083713.
(20) Lavrov, E. V.; Herklotz, F.; Weber, J. *Phys. Rev. B* **2009**, *79*, 165210.
(21) Lavrov, E. V.; Herklotz, F.; Weber, J. *Phys. Rev. Lett.* **2009**, *102*, 185502.
(22) You, J. B.; Zhang, X. W.; Cai, P. F.; Dong, J. J.; Gao, Y.; Yin, Z. G.; Chen, N. F.; Wang, R. Z.; Yan, H. *Appl. Phys. Lett.* **2009**, *94*, 262105.
(23) Studenikin, S. A.; Golego, N.; Cocivera, M. *J. Appl. Phys.* **2000**, *87*, 2413.
(24) Dev, A.; Niepelt, R.; Richters, J. P.; Ronning, C.; Voss, T. *Nanotechnology* **2010**, *21*, 065709.
(25) Meyer, B. K.; Alves, H.; Hofmann, D. M.; Kriegseis, W.; Forster, D.; Bertram, F.; Christen, J.; Hoffmann, A.; Straβburg, M.; Dworzak, M.; Haboeck, U.; Rodina, A. V. *Phys. Status Solidi B* **2004**, *241*, 231.
(26) Teke, A.; Özgür, Ü.; Dogan, S.; Gu, X.; Morkoç, H.; Nemeth, B.; Nause, J.; Everitt, H. O. *Phys. Rev. B* **2004**, *70*, 195207.
(27) Aminzadeh, A.; Sarikhani-fard, H. *Spectrochim. Acta, Part A* **1999**, *55*, 1421.
(28) Cuscó, R.; Alarcón-Lladó, E.; Ibáñez, J.; Artús, L.; Jiménez, J.; Wang, B.; Callahan, M. J. *Phys. Rev. B* **2007**, *75*, 165202.
(29) Windisch, C. F., Jr.; Exarhos, G. J.; Yao, C.; Wang, L. Q. *J. Appl. Phys.* **2007**, *101*, 123711.
(30) Kaschner, A.; Haboeck, U.; Strassburg, Mar.; Strassburg, Mat.; Kaczmarczyk, G.; Hoffmann, A.; Thomsen, C.; Zeuner, A.; Alves, H. R.; Hofmann, D. M.; Meyer, B. K. *Appl. Phys. Lett.* **2002**, *80*, 1909.
(31) Reuss, F.; Kirchner, C.; Gruber, Th.; Kling, R.; Maschek, S.; Limmer, W.; Waag, A.; Ziemann, P. *J. Appl. Phys.* **2004**, *95*, 3385.
(32) Friedrich, F.; Nickel, N. H. *Appl. Phys. Lett.* **2007**, *91*, 111903.
(33) Sann, J.; Stehr, J.; Hofstaetter, A.; Hofmann, D. M.; Neumann, A.; Lerch, M.; Haboeck, U.; Hoffmann, A.; Thomsen, C. *Phys. Rev. B* **2007**, *76*, 195203.
(34) Bundesmann, C.; Ashkenov, N.; Schubert, M.; Spemann, D.; Butz, T.; Kaidashev, E. M.; Lorenz, M.; Grundmann, M. *Appl. Phys. Lett.* **2003**, *83*, 1974.
(35) Kennedy, J.; Sundrakannan, B.; Katiyar, R. S.; Markwitz, A.; Li, Z.; Gao, W. *Curr. Appl. Phys.* **2008**, *8*, 291.
(36) Serrano, J.; Romero, A. H.; Manjón, F. J.; Lauck, R.; Cardona, M.; Rubio, A. *Phys. Rev. B* **2004**, *69*, 094306.
(37) Manjón, F. J.; Marí, B.; Serrano, J.; Romero, A. H. *J. Appl. Phys.* **2005**, *97*, 053516.

AM100298P